https://doi.org/10.33271/nvngu/2024-5/130

I. V. Vassiliyev[1],
orcid.org/0000-0002-6216-0443,
B. B. Imansakipova[*2],
orcid.org/0000-0003-0658-2112,
Sh. K. Aitkazinova[2],
orcid.org/0000-0002-0964-3008,
K. Z. Issabayev[3],
orcid.org/0000-0001-5183-3668,
M. K. Olzhabayev[3],
orcid.org/0000-0002-2741-6562,
D. G. Kanapiyanova[2],
orcid.org/0000-0003-2819-3791

1 – Special Design and Technology Bureau "Granit", Almaty, the Republic of Kazakhstan
2 – Satbayev University, Almaty, the Republic of Kazakhstan
3 – Military Engineering Institute of Radio Electronics and Communications, Almaty, the Republic of Kazakhstan
* Corresponding author e-mail: imansakipovakazntu@gmail.com

FREQUENCY DEPENDENCE OF REFLECTIONS ON RADAR LANDMARKS

Purpose. Reducing the dispersion of radar reflections from local objects, with multi-frequency sensing, to solve the problem of orientation by radar reflections from objects.

Methodology. Reflections from local objects in the entire frequency range of the radar station (RS) at the same radio engineering position were measured by three independent radars of the same type on different days and at different antenna elevations. The deviation of the radar stations in the position did not exceed 500 meters. Coordinates (azimuth, range) of reflections of several separate local objects were allocated for each radar. The average values of reflections from local objects and their dispersion in the frequency range were calculated. Using various algorithms, individual frequencies were sampled and the reflected signals were averaged at these frequencies. The decrease in the dispersion of the reflected signal from the number of frequencies at which reflections were measured and from the algorithm for selecting these frequencies was investigated.

Findings. Averaging the values of reflections from local objects for several frequencies leads to a decrease in dispersion and, as a result, to a more accurate correspondence of the reflected signal level to the geometric size of the local object. The variance decreases most rapidly for a small number of frequencies selected for averaging when selecting frequencies located in an interval of at least 1% relative to each other.

Originality. To solve the problem of orientation based on radar reflections from local objects, it is necessary to identify the landmarks selected on a digital terrain model. Due to the fact that local objects (hills) are a collection of many reflectors falling into the allowed volume of the radar, with different levels of reflections and random phases, there may not be radar reflection from a local object at a certain frequency, or it may be very small. In order to unambiguously identify all landmarks, measurements must be carried out at several frequencies. The work has established how many frequencies measurements should be performed at and on what principle these frequencies should be selected.

Practical value. The advent of digital terrain models made it possible to solve the problem of terrain orientation by comparing radar reflections from local objects with reflection models based on digital terrain maps. Radar reflection models use mathematical expectations of reflection values, unlike real reflections, which have random deviations in signal levels depending on the operating frequency. Reducing the variance of these deviations increases the accuracy of identifying characteristic local objects (landmarks) used to orient the radar in the absence of data from satellite navigation systems.

Keywords: *dispersion, radar, frequency range, landmark, digital terrain model*

Introduction. The advent of global navigation Systems (GNSS) would seem to have solved most of the problems of navigation support for various applications. The relevance and importance of these navigation systems for science and society are undeniable [1]. However, the signals of these navigation systems near the Earth's surface are so weak that they are easily suppressed by natural or artificial interference. At the same time, the most popular GNSS signals offered with unlimited access are not encrypted or authenticated, which allows them to be forged [2].

Problem statement. The need to ensure navigation, in the absence of GNSS signals or their distortion, set the task of finding alternative options for determining coordinates and orientation to the cardinal directions. One of these directions was the revival of ultra-long-wave radio navigation systems such as Loran D [3], although these systems are expensive, require maintenance and do not have sufficient positioning accuracy. The emergence of sufficiently accurate and accessible digital terrain models (DEM), which were obtained in the topographic mission of the space Shuttle (Shuttle Radar Topography Mission, SRTM), provided new opportunities, for example, to track the dynamics of terrain [4]. Of course, digital models have certain disadvantages, such as the presence of areas with uncertain heights, especially in mountainous areas, but the use of emission and void filtration methods [5] allows increasing the accuracy of terrain models.

There is a promising opportunity to use digital terrain models as reference points for navigation based on radar reflections from the terrain. The work [6] presents the results of experiments on terrain orientation using a small and cheap marine radar. The results of reflections from buildings, highways, parking lots, large and medium-sized lampposts, from soil with grass and trees were obtained – all within a radius of several kilometers. For confident orientation, it is necessary to solve the problem of building a radar reflection model based on DEM, taking into account the technical features of the radar, such as the peculiarities of the antenna pattern and its pulse (resolved) volume. During radar sensing of the terrain, the radar simultaneously receives a variety of signals reflected from various areas of the terrain that fall within the allowed volume. These signals, which have amplitudes and phases independent of each other for different operating frequencies of the radar, are summed up in the receiving device and the total signal, in general, has a random value. Even high elevations at certain frequencies can give a slight radar response, which can lead to the "disappearance" of landmarks for the radar.

One possible way to solve this problem is to measure radar reflections at several radio frequencies. In the work, based on

experimental data, the possibilities of obtaining frequency-averaged radar reflections were considered in order to more adequately match them to radar terrain models based on digital terrain models.

Literature review. Reflections from local objects have always been a problem for radar. The study of reflections from local objects that interfered with the reception of reflections from aerial targets was one of the important tasks of radar. In order to combat interference from reflections from the earth's surface and mountains, systematic studies were conducted in different frequency ranges. D. Barton made a great experimental and theoretical contribution to the study of this problem. The studies were conducted with different types of terrain (plain, mountains, industrial buildings) and in different frequency ranges. They showed a wide range of values of the effective scattering surface depending on specific areas of the terrain and the frequency range. It was concluded that the value of the mathematical expectation of reflections from local objects depends on their height to the fourth degree. At low viewing angles, the frequency dependence of the reflected signal level is extremely high, which made modeling reflections from local objects at a specific frequency almost impossible.

The backscattering dispersion decreases with an increase in the operating frequency of the radar, but practically does not depend on the polarization of the signal and the resolved (pulse) volume. With small frequency changes, statistical patterns do not change, which suggests that when averaging backscattering diagrams at several independent frequencies, it is possible to obtain reflection values close to the median value.

Many researchers have attempted to detect patterns in reflections depending on the type of terrain, frequencies, and polarization. In [7], using the method of moments (MoM) and applying the Kullback-Leibler divergence test, it was found that the logarithmically normal distribution is the best match for measurements of the amplitude of reflections from urban buildings, whereas measurements of reflection amplitudes in rural areas best correspond to the K-distribution. It was shown in [8] that the signal reflected from the earth's surface changes over time due to changes in the earth, and backscattering (RCS) can be approximated by various distributions, such as Rayleigh distribution, Rice distribution, lognormal distribution or Weibull distribution, depending on different types of soil. A map with four types of terrain was modeled, including deserts, farms, hills and cities, with which distributed reflections from the ground were formed using empirical scattering coefficients, different for each type of vegetation cover. As a result of experiments using the modeling procedure, it is shown that in each type of terrain of all four types of landscapes, the distribution of the amplitude of reflections actually obeys the Rayleigh model.

However, in [9] a method was proposed for modeling interference from local objects, in which the reflections of radar signals distributed over the ground are formed using a spatial correlated model of the backscattering coefficient. In this model, unlike previous works, the amplitude of reflections is not Rayleigh-distributed, and the spectral power density obeys the Gaussian distribution. Specifically, the Weibull distribution is used for the amplitude of reflections on runways, and the logarithmically normal distribution is used for the amplitude of reflections on meadows. Experiments with millimeter-wave radar have shown sufficient effectiveness of the model. In [10], an artificial neural network was used to classify four common models of radar reflections from local objects (Gaussian, Weibull, Rayleigh, and K-distribution), with the help of which such important distribution characteristics as asymmetry and kurtosis were extracted.

Slightly better results of radar reflection modeling, suitable for orientation purposes, are obtained when modeling the sea-land boundary. With abnormal propagation of radio waves and the formation of waveguide structures over the sea, real reflections can differ greatly from simulated reflections at small angles above the sea surface. Although there are relatively accurate models of reflections from the sea surface [11] that predict the average levels of backscattering of radio waves depending on wind speed and direction, sea conditions (wave height), radar frequency, glide angle, etc., but in practice it is almost impossible to obtain these data with acceptable accuracy, affecting the signal level. At the same time, for aviation radars that survey the surface at greater angles than ship radars, a method for calculating the reflection coefficients of radio waves was developed [12], which showed good results during flight tests.

It is shown that the use of digital terrain models (DEM) [13] significantly improves the ability to orient ships according to onboard radar readings. Using artificial intelligence to isolate support vectors (SVM) [14], good results were obtained on the separation of reflections from land and sea surfaces according to 9 signs given in this work. The patent [15] proposes a method for identifying landmarks in radar reflections, used to assess the energy potential of radar stations, which allows you to identify radar landmarks located behind the radio horizon against the background of receiver noise and external interference.

Unsolved aspects of the problem. Different approaches are used to solve the problem of modeling radar reflections from local objects based on digital terrain models (DEM), for example, [16–18] and others. All of them are based on various statistical reflection models and the resulting reflection models cannot unambiguously coincide with real reflections. Of course, increasing the accuracy of digital terrain models increases the accuracy of radar reflection models, but not so significantly. Recently, the most popular models of radar reflections are the SRTM 30 m digital terrain model and the GlobeLand30 dataset, which are freely available [19].

If it is impossible to accurately simulate reflections from local objects, a number of researchers are trying to solve the problem of obtaining radar reflections less susceptible to random factors. One of the methods [20] is the accumulation of radar reflections in different time periods, in which different external conditions affect radar reflections. Another way is to measure interfering reflections at different frequencies [21]. The authors used this method to reduce the influence of multipath interference inside buildings. It has shown good results in reducing dispersion, and could be useful for solving radar navigation problems.

Purpose. The purpose of this work was to study the dependence of the levels of radar signals reflected from hills (hills, mountains), which can be used as landmarks, at various frequencies. The possibility of reducing the dispersion of the RCS of radar landmarks by averaging the measurement results obtained at different frequencies was investigated.

To achieve these goals, it was necessary to solve several tasks:

- substantiation of the research methodology and the technical means involved;
- measuring the levels of the reflected signal of control local objects in the entire range of operating frequencies of radar stations;
- assessment of the effect of the antenna lift height on the nature of the frequency dependence of the signals reflected from the landmarks;
- assessment of the effect of the angular displacement of the antenna on the nature of the frequency dependence of the signals reflected from the landmarks;
- calculation of the average values of the reflected signal levels and their dispersion over the entire frequency range;
- calculation of the average values of the reflected signal levels for limited frequency samples, for different sample sizes and the principles of their selection;
- performing an analysis of the experimental data obtained.

Description of the methodology (structure, sequence) of the research. Two meter-wave range (VHF) radars of the P-18M and P-18K models were used to conduct the experiments. This wave range is characterized by a very large dispersion of the levels of signals reflected from the ground. The appearance of the radars is shown in Fig. 1.

Fig. 1. The appearance of the radar P-18M (P-18K)

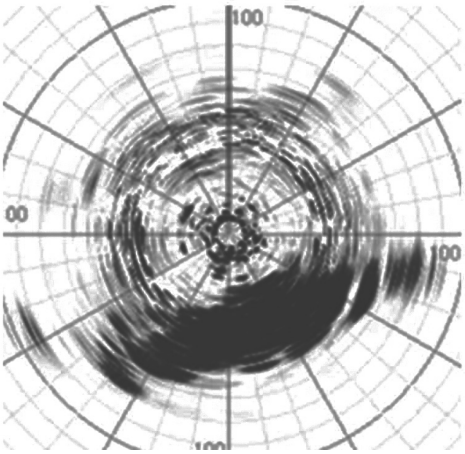

Fig. 2. An example of reflections from local objects of VHF radars in the experiments of the authors

The main technical characteristics of the radar P-18M (P-18K):

- the type of radiation is pulsed;
- the duration of the partial pulse is 6 microseconds;
- ADC clock (ADC) 2 microseconds;
- operating frequency range 140–170 MHz;
- frequency tuning step 250 kHz;
- output power of 8 kW;
- the width of the antenna pattern in the horizontal plane is 8°;
- the noise coefficient of the receiving device is 1 dB.

The P-18K radar, unlike the P-18M radar, uses an 18-bit analog-to-digital converter (ADC) instead of a 12-bit ADC. The relative width of the radar frequency range (Band) is equal to (170 – 140)/155 = 0.19 (19 %).

The measurements were carried out in the period from May to August 2023 at one radio engineering position in the area of the northern slope of the mountains of the Trans-Ili Alatau (Kazakhstan). The distance between the radars is 200 meters. Measurements on the P-18K radar were carried out at heights of the antenna phase center similar to the height of the P-18M radar antenna (about 6 meters above ground level) and at an increased antenna height. In total, 3 series of measurements were made over the entire frequency range of the radars.

On the recordings of radar reflections, separate contrasting objects suitable for use as landmarks were identified, their coordinates (azimuth and distance) were determined, and for these coordinates the amplitudes of the reflected signal at all operating frequencies of the radar were measured in ADC units.

Fig. 2 shows an example of the appearance of radar indicators obtained in the experiments of the authors.

As can be seen from Fig. 2, reflections from many local objects "merge" on the all-round view indicator with each other due to the fact that the reflections of several local objects (hills) fall into the main maximum of the radiation pattern. Nevertheless, on the all-round view screens, it is possible to identify individual reflections that are close in angular dimensions to the width of the radar radiation pattern (contrasting objects), which can be used to study frequency dependencies.

For the selected landmarks, the averaged values of the reflected signal level for all frequencies and the RMS values of this signal from the median value were calculated. Then, samples of signals for different frequencies and averaging of reflected signals in these samples were made from the total data array for each of the landmarks. The decrease in the dispersion of the reflected signal from the number of frequencies at which reflections were measured (sample size) was investigated.

Results. Fig. 3 shows the reflected signal levels obtained on the P-18K radar with an antenna phase center height of about 6 meters for 4 local objects (objects) suitable for use as landmarks. As can be seen from Table 1, object 5, the reflections from which are shown in Fig. 5, and object 2 are essentially the same landmark (azimuth 23.550), only signal levels were measured in neighboring radar resolution elements at a range (–300 meters). The red dots indicate the frequencies at which reflection measurements could not be performed due to interference. The reflection levels are interpolated by a linear function based on the results of measurements at adjacent frequencies at which measurements were made.

The coordinates of the objects are shown in Table 1. Also in Table 1 are the average values of the average reflected signal levels (Amax) and the standard deviations of the reflected signal amplitude (Sigma) from the average value in ADC units and percentages (%).

Fig. 3 shows that the number of frequencies at which the reflected signal level from objects decreases significantly (by more than 20 dB) relative to the average value may be 16 out of 121 radar operating frequencies (13.2 %). At the same time, the nature of the dependence of the reflected signal level on the frequency is different for different local objects. The maxima of reflected signals from different objects are observed at different frequencies, which allows us to conclude that the

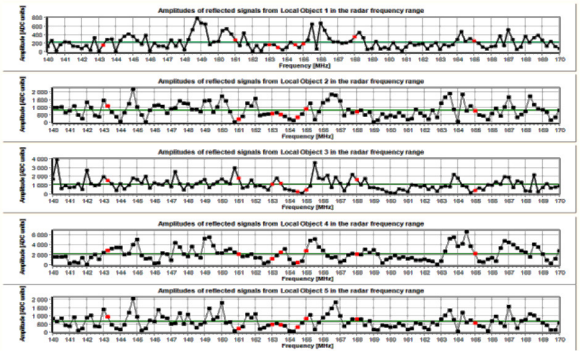

Fig. 3. Frequency dependence of the reflected signal levels for landmarks measured by the P-18K radar at an antenna height of 6 meters

Table 1

Coordinates of landmarks (objects) and average signal levels for an antenna at a height of 6 meters

Number of frequencies with interference 8

№ LO	Range [km]	Azimuth [degrees]	Amax [ADC units]	Sigma [ADC units]	Sigma [%]
1	75,3	270,00	225	158	70,16
2	78,0	23,55	816	473	57,98
3	63,0	284,77	1108	677	61,13
4	58,2	334,16	2210	1 390	62,91
5	77,7	23,55	650	402	61,83

frequency-dependent contribution of radar equipment to the measurement results is relatively small.

In the next experiment, the height of the antenna phase center was increased by 2.5 meters and the levels of the reflected signal from the same landmarks were measured (Fig. 4) over the entire operating frequency range. Table 2 shows the average levels of reflected signals and their standard deviations calculated for the entire frequency range.

An increase in the height of the antenna above ground level by 1.42 times led to an increase in both the average levels of the reflected signal from all local objects (landmarks) and the maximum values of the reflected signals by about 6 dB. The nature of the frequency dependence of the reflected signals has not changed significantly. The magnitude of the RMS deviations of the reflected signals in the frequency band has been preserved (at about 60 %).

At the third stage of the experiment, measurements were carried out using the P-18M radar with the height of the antenna phase center 7 meters above ground level. The position of the radar was shifted relative to the position of the P-18K radar by about 300 meters, which corresponds to one discrete measurement of the radar range. Other landmarks were selected for the experiment. The distance to them is 1.5–2 times greater than in previous experiments. The measurement results are shown in Fig. 5. Table 3 shows the levels of reflected signals and their RMS deviations in the frequency range.

Increasing the distance to local objects naturally led to a decrease in the levels of reflected signals, and increased the standard deviations. This is probably caused by a decrease in the signal-to-noise ratio, since the standard deviations increase markedly with a decrease in the average value of the reflected signal level.

Further experiments were carried out by post-processing the results obtained with the help of radars. The following types of processing were applied to all received radar images. However, the article provides as an example only the results obtained by the P-18K radar with an antenna elevation of 8.5 meters, since radar reflections from local objects had the best signal/(noise + interference) ratio, and there were a small number of operating frequencies at which a high level of interference was observed.

Since, when measuring radar reflections at an arbitrarily selected frequency, as shown above, the probability that a local

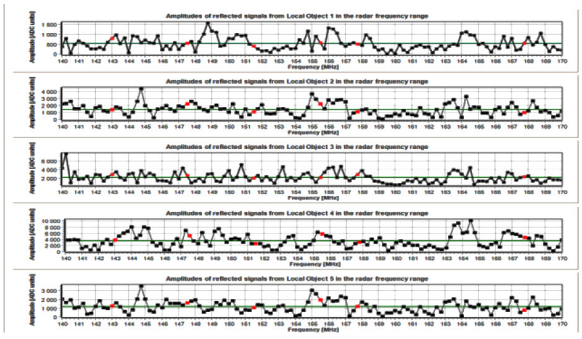

Fig. 4. Frequency dependence of the reflected signal levels for landmarks measured by the P-18K radar at an antenna height of 8.5 meters

Table 2

Coordinates of landmarks (objects) and average signal levels for an antenna at an altitude of 8 meters

Number of frequencies with interference 6

№ LO	Range [km]	Azimuth [degrees]	Amax [ADC units]	Sigma [ADC units]	Sigma [%]
1	75,3	269,30	525	322	61,42
2	78,0	23,20	1439	797	55,42
3	62,7	284,24	2162	1 195	55,28
4	58,2	333,63	3494	2 125	60,82
5	77,7	23,38	1205	648	53,80

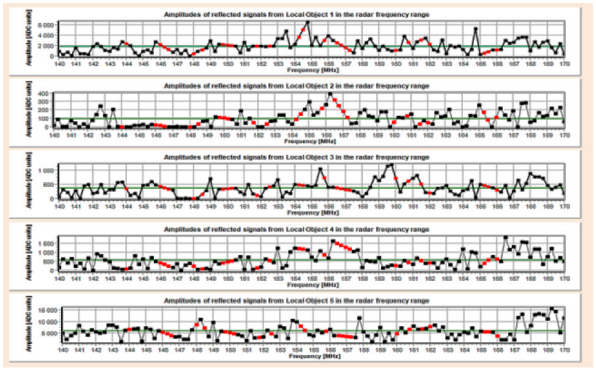

Fig. 5. Frequency dependence of the reflected signal levels for landmarks measured by the P-18M radar at an antenna height of 7 meters

Table 3

Coordinates of landmarks (objects) and average signal levels for an antenna at an altitude of 7 meters

Number of frequencies with interference 25

№ LO	Range [km]	Azimuth [degrees]	Amax [ADC units]	Sigma [ADC units]	Sigma [%]
1	105,3	98,44	1859	1 166	62,70
2	145,8	62,93	96	86	89,52
3	114,9	95,45	374	242	64,76
4	116,7	256,99	580	421	72,61
5	82,5	216,56	5983	2 978	49,77

object (landmark) will not be detected may be 13.2 %, the question of the number of radar reflections that need to be obtained at several frequencies in order to increase the probability of guaranteed detection of landmarks was investigated. By reducing the standard deviation of the measured signals relative to the average values, the probability that the measured signal may be below the noise level should decrease. To do this, 200 groups of data samples were randomly made from each data array for previously selected landmarks, simulating measurements at randomly selected frequencies. The values obtained were averaged in each sample, and these averaged results were compared with the average frequency reflection level for this local landmark calculated earlier (Tables 1–3). The sample size ranged from 1 to 20 randomly selected values (freq. number). Table 4 below shows the results obtained for

Table 4

Dependence of the standard deviation of the sample averages on the median value for different sample sizes (volumes)

Freq. number	Asr200 [ADC units]	Sigma [ADC units]	Sigma [%]
1	486	315	64,85
2	536	239	44,60
3	519	187	36,01
4	519	151	29,07
5	513	142	27,64
6	529	132	24,89
7	522	126	24,18
8	520	111	21,42
9	508	107	20,97
10	520	103	19,76
11	516	93	17,98
12	511	92	18,03
13	525	86	16,42
14	518	86	16,67
15	523	84	16,07
16	534	81	15,12
17	522	85	16,34
18	528	79	15,00
19	524	72	13,69
20	532	71	13,44

the local landmark No. 1 with coordinates: azimuth 267.20, distance 78.3 km. The values averaged over 200 sample groups (Asr200) are hereinafter referred to as median values.

These data show that the RMS values decrease in proportion to the square root of the sample size (freq. number), which is typical for the normal distribution law.

The following table (Table 5) shows the results of similar calculations (RMS deviations of the averaged signal levels) with a random selection of the initial frequency of the first sample element. The remaining sample elements were taken with regular frequency shifts from 0.25 to 5.0 MHz from each other, unlike previous calculations in which the samples were random.

Unlike Table 4, Table 5 shows the values for a sample of two elements in the first row. Therefore, when comparing the data shown in Tables 4 and 5, a shift in sample sizes by 1 value should be taken into account.

Analyzing the calculation results shown in Table 5, we can note that the values of standard deviations of less than 30 % begin to prevail already in the 3rd row of the table corresponding to the averaging of signals at 4 frequencies. At the same time, the increase in the interval between frequencies ("step", vertical columns), and a decrease in the standard deviation is also observed. For a frequency range of 1.5 MHz with 4 frequency samples (3 lines), the decrease in the RMS value with respect to the 0.25 MHz step is 42.95/27.97 = 1.54 times. And this trend is observed for all sample sizes over 3.

As the sample size increases (the number of frequencies for measuring reflections), the standard deviation decreases. In line 7, corresponding to the sample size of 8 frequencies (a 2-fold increase in the sample size), in most cases the standard deviations do not exceed 21 %, which is 2 times less than the increase in the sample size.

Very similar results were obtained for other radars and local landmarks, which made it possible to draw generalizing conclusions from the data provided and obtain the numerical values given in the conclusions.

Conclusions. Based on the results of experimental studies and modeling, the following conclusions can be drawn:

1. Averaging reflections at several frequencies reduces the dispersion of the levels of reflected signals from local landmarks and the probability of their not being detected.

2. Measuring at 4 frequencies or more reduces the standard deviation to less than 30 %.

3. The choice of random frequencies with an interval of at least 1 % (1.5 MHz) relative to each other reduces the standard deviation of the average sample signal relative to the median value by 25 % or more.

In this work, the statistical characteristics of reflections from local landmarks located at distances greater than the radio horizon were studied

$$R(\text{km}) \geq 3.57\sqrt{h_a(\text{m})},$$

where R is the distance to the horizon; h_a – the height of the antenna phase center elevation above ground level.

At these distances, there are no problems with separating signals from local landmarks (mountains, hills) from reflections from the flat terrain. However, since the accuracy of determining the azimuth depends on the width of the antenna pattern, the accuracy of the location is directly related to the distance to the landmarks. As these distances decrease, the accuracy of determining coordinates increases, but interference signals reflected from the flat terrain appear.

Taking into account the results of the research obtained during the experiment, the specific levels of reflections from elevations in the VHF range exceed the reflections of signals from fields by 20 dB or more. It is of interest to create an algorithm for identifying radar landmarks against the background of interference from a slightly hilly earth. We consider it promising to use the correlation methods proposed in the patent [22], as well as the construction of mathematical models for analyzing the amplitude-frequency spectrum of the reflected signal [23].

Table 5

Dependence of the standard deviation of the sample averages on the median value for different sample sizes (freq. number) at fixed frequency steps

Freq Number/Step	0,25	0,50	0,75	1,00	1,25	1,50	1,75	2,00	2,25	2,50	2,75	3,00	3,25	3,50	3,75	4,00	4,25	4,50	4,75	5,00
1	48,17	48,23	44,10	41,73	46,56	44,20	43,79	45,71	44,99	40,76	36,63	36,16	38,95	40,02	40,05	39,02	41,88	36,00	38,37	44,35
2		46,51	43,68	39,43	35,53	35,65	33,13	36,56	33,70	32,12	31,13	33,25	36,08	34,70	34,07	35,47	32,58	32,38	29,33	33,26	32,69
3		42,95	36,30	33,58	31,12	28,19	27,97	29,38	30,68	26,22	32,33	29,79	28,93	22,87	24,99	28,06	26,67	21,62	19,39	22,56	26,38
4		40,53	32,44	26,93	26,33	22,87	22,96	26,70	29,11	23,75	29,01	23,72	24,91	17,75	21,06	19,50	21,17	24,26	21,34	20,97	27,22
5		35,98	29,17	24,27	21,36	21,31	24,24	22,89	26,57	17,61	24,89	18,07	20,43	17,15	20,82	22,78	21,48	22,80	18,96	22,39	23,89
6		36,04	30,64	28,94	20,44	20,62	22,21	22,33	25,08	11,27	20,31	16,19	18,96	18,16	21,92	21,34	21,48	24,67	21,22	21,57	25,30
7		34,65	24,98	17,16	19,31	20,16	20,14	20,08	21,01	11,40	18,85	17,23	16,84	16,85	19,53	20,79	22,09				
8		31,64	23,42	16,21	19,23	17,70	17,70	17,22	19,45	12,31	20,79	17,02	17,69	17,09	21,53						
9		31,68	21,00	16,03	18,75	16,37	17,22	14,36	19,32	12,56	19,46	18,08	18,07	17,87							
10		29,76	19,74	15,53	15,80	14,74	17,61	13,71	20,00	12,91	19,72	16,68	18,79								
11		27,90	17,22	15,46	16,42	12,97	15,82	15,60	18,66	11,12	19,78										
12		26,43	17,86	14,30	14,10	12,78	15,91	14,36	20,24	12,58	20,34										
13		22,49	16,27	14,50	15,72	12,05	15,42	12,84	19,21	12,26											
14		25,21	15,49	13,48	13,92	12,32	14,41	14,49	19,41												
15		23,07	15,79	13,80	13,09	9,84	13,45	12,96													
16		22,15	15,79	12,53	12,82	10,37	15,97	14,04													
17		21,19	16,42	11,30	12,10	8,53	15,11														
18		18,61	15,35	10,79	12,35	9,16															
19		18,22	15,33	10,04	11,32	8,38															
20		15,35	14,35	9,96	10,75	9,07															

Acknowledgements. *This article is based on the results of research on the topic "Development of methods of ground-based radar navigation" IRN No. AP148036/0222.*

References.

1. Langley, R. B., Teunissen, P. J., & Montenbruck, O. (2017). Introduction to GNSS. In Teunissen, P. J., Montenbruck, O. (Eds.). *Springer Handbook of Global Navigation Satellite Systems*. Springer Handbooks. Springer, Cham. https://doi.org/10.1007/978-3-319-42928-1_1.

2. Humphreys, T. (2017). Interference. In Teunissen, P. J., Montenbruck, O. (Eds.). *Springer Handbook of Global Navigation Satellite Systems*. Springer Handbooks. Springer, Cham. https://doi.org/10.1007/978-3-319-42928-1_16.

3. Lo, S. C., Peterson, B. B., Hardy, T., & Enge, P. K. (2010). Improving Loran Coverage with Low Power Transmitters. *Journal of Navigation, 63*(1), 23-38. https://doi.org/10.1017/S0373463309990245.

4. LaLonde, T., Shortridge, A., & Messina, J. (2010). The Influence of Land Cover on Shuttle Radar Topography Mission (SRTM) Elevations in Low-relief Areas. *Transactions in GIS, 14*, 461-479. https://doi.org/10.1111/j.1467-9671.2010.01217.x.

5. Mukul, M., Srivastava, V., Jade, S., & Mukul, M. (2017). Uncertainties in the Shuttle Radar Topography Mission (SRTM) Heights: Insights from the Indian Himalaya and Peninsula. *Scientific Reports, 7*, 41672. https://doi.org/10.1038/srep41672.

6. Galati, G., & Pavan, G. (2018). Generation of Land-Clutter Maps for Cognitive Radar Technology. In Rocha, Á., Adeli, H., Reis, L., Costanzo, S. (Eds.) Trends and Advances in Information Systems and Technologies. WorldCIST'18 2018. *Advances in Intelligent Systems and Computing, 746*. Springer, Cham. https://doi.org/10.1007/978-3-319-77712-2_141.

7. Melebari, A., Abdul Gaffar, M. Y., & Strydom, J. J. (2015). Analysis of high resolution land clutter using an X-band radar. *2015 IEEE Radar Conference*, Johannesburg, South Africa, (pp. 139-144). https://doi.org/10.1109/RadarConf.2015.7411869.

8. Wang, X., Wang, H., Yan, S., Li, L., & Meng, C. (2012). Simulation for surveillance radar ground clutter at low grazing angle. *2012 International Conference on Image Analysis and Signal Processing*, Huangzhou, China, (pp. 1-4). https://doi.org/10.1109/IASP.2012.6424999.

9. Qin, F., Wan, Y., Liang, X., & Zhou, S. (2019). Clutter Modeling for FOD Surveillance Radar at Low Grazing Angle. *IEEE International Conference on Signal, Information and Data Processing (ICSIDP)*, Chongqing, China, (pp. 1-4). https://doi.org/10.1109/ICSIDP47821.2019.9173431.

10. Darzikolaei, M. A., Ebrahimzade, A., & Gholami, E. (2015). Classification of radar clutters with Artificial Neural Network. *2nd International Conference on Knowledge-Based Engineering and Innovation (KBEI)*, Tehran, Iran, (pp. 577-581). https://doi.org/10.1109/KBEI.2015.7436109.

11. Maria S. Greco, & Watts, S. (2014). Chapter 11 – Radar Clutter Modeling and Analysis. In Nicholas D. Sidiropoulos, Fulvio Gini, Rama Chellappa, Sergios Theodoridis (Eds.). *Academic Press Library in Signal Processing, 2*, 513-594. https://doi.org/10.1016/B978-0-12-396500-4.00011-9.

12. Kim, T.-H., Jeon, H.-W., Park, S.-H., Park, J.-T., Jung, C.-H., Park, J.-H., & Bae, J. (2021). Development of Ground Clutter Re-

flectivity Calculation Methods and Simulated Ground Clutter Signal Generation Models Using Airborne Radars. *Journal of Electromagnetic Engineering and Science, 32*(6), 541-548. https://doi.org/10.5515/KJKIEES.2021.32.6.541.
13. Wu, Q., & Zhang, W. (2014). Modeling and simulation of airborne radar clutter in a littoral complex environment. *2014 IEEE International Conference on Communiction Problem-solving*, Beijing, China, (pp. 496-499). https://doi.org/10.1109/ICCPS.2014.7062331.
14. Zhang, L., Xue, A., Zhao, X., Xu, S., & Mao, K. (2021). Sea-Land Clutter Classification Based on Graph Spectrum Features. *Remote Sensing, 13,* 4588. https://doi.org/10.3390/rs13224588.
15. Baturina, E. B., & Vasiliev, I. V. (2011). *Method for assessing the energy potential of a radar station,* (Patent No. 25343 RK: MPK8 G 01S 7/40/) the Kyrgyz Republic.
16. Li, H., Wang, J., Fan, Y., & Han, J. (2018). High-Fidelity Inhomogeneous Ground Clutter Simulation of Airborne Phased Array PD Radar Aided by Digital Elevation Model and Digital Land Classification Data. *Sensors, 18*, 2925. https://doi.org/10.3390/s18092925.
17. Kurekin, A., Radford, D., Lever, K., Marshall, D., & Shark, L.-K. (2011). New method for generating site-specific clutter map for land-based radar by using multimodal remote-sensing images and digital terrain data. *IET Radar, Sonar & Navigation, 5(3)*, 374-388, https://doi.org/10.1049/iet-rsn.2010.0036.
18. Wang, A., Zhang, W., & Cao, J. (2012). Terrain clutter modeling for airborne radar system using digital elevation model. *The 2012 International Workshop on Microwave and Millimeter Wave Circuits and System Technology*, Chengdu, China, (pp. 1-4). https://doi.org/10.1109/MMWCST.2012.6238182.
19. Shasha, L. (2013). The study of radar ground clutter simulation based on DEM. *2013 IEEE International Conference on Information and Automation (ICIA)*, Yinchuan, China, (pp. 258-262). https://doi.org/10.1109/ICInfA.2013.6720306.
20. Kim Donghoon, Park, A.J., Suh, U.-S., Goo, D., Kim Dongwan, Yoon, B., Fa, W.-S., & Kim, S. (2022). Accurate Clutter Synthesis for Heterogeneous Textures and Dynamic Radar Environments. *IEEE Transactions on Aerospace and Electronic Systems, 58*(4), 3427-3445. https://doi.org/10.1109/TAES.2022.3151585.
21. Mendakulov, Zh. K., Morosi, S., Martinelli, A., & Isabaev, K. Zh. (2021). Investigation of the possibility of reducing errors in determining the coordinates of objects indoors by multi- frequency method. *Naukovyi Visnyk Natsionalnoho Hirnychoho Universytetu*, (1), 137-144, https://doi.org/10.33271/nvngu/2021-1/137.
22. Sdvyzhkova, O., Golovko, Y., Dubytska, M., & Klymenko, D. (2016). Studying a crack initiation in terms of elastic oscillations in stress strain rock mass. *Mining of Mineral Deposits, 10*(2), 72-77.

Частотна залежність відображень від радіолокаційних орієнтирів

І. В. Васильєв[1], *Б. Б. Імансакіпова*[*2], *Ш. К. Айтказінова*[2], *К. Ж. Ісабаєв*[3], *М. К. Олжабаєв*[3], *Д. Г. Канапіянова*[2]

1 – Спеціальне конструкторсько-технологічне бюро «Граніт», м. Алмати, Республіка Казахстан
2 – НАТ «Казахський національний дослідницький технічний університет імені К. І. Сатпаєва», м. Алмати, Республіка Казахстан
3 – Військово-інженерний інститут радіоелектроніки та зв'язку, м. Алмати, Республіка Казахстан
* Автор-кореспондент e-mail: imansakipovakazntu@gmail.com

Мета. Зниження дисперсії радіолокаційних відображень від місцевих предметів, при багаточастотному зондуванні, для вирішення завдання орієнтування за радіолокаційними відображеннями від предметів.

Методика. Трьома незалежними однотипними радіолокаторами в різні дні та за різних висот підйому антени були виміряні відображення від місцевих предметів у всьому діапазоні частот радіолокаційної станції (РЛС) на одній радіотехнічної позиції. Відхилення місць стояння радіолокаторів на позиції не перевищувало 500 метрів. Для кожного радіолокатора виділялися координати (азимут, дальність) відображень декількох окремо розташованих місцевих предметів. Розраховувалися середні значення відображень від місцевих предметів і їх дисперсії в діапазоні частот. Із використанням різних алгоритмів проводилася вибірка окремих частот і усереднення відбитих сигналів на цих частотах. Досліджувалося зниження дисперсії відбитого сигналу в залежності від кількості частот, на яких вимірювалися відображення, і від алгоритму вибору цих частот.

Результати. Усереднення величин відображень від місцевих предметів для декількох частот призводить до зниження дисперсії і, як наслідок, до більш точної відповідності рівня відбитого сигналу геометричному розміру місцевого предмета. Найбільш швидко дисперсія знижується для малої кількості частот, обраних для усереднення, при виборі частот, розташованих в інтервалі не менше 1 % один щодо одного.

Наукова новизна. Для вирішення завдання орієнтування за радіолокаційними відображеннями від місцевих предметів необхідна ідентифікація орієнтирів, обраних на цифровій моделі рельєфу місцевості. Через те, що місцеві предмети (височини) являють собою сукупність безлічі відбивачів, що потрапляють до допустимого обсягу РЛС, із різними рівнями відображень і випадковими фазами, то радіолокаційного відображення від місцевого предмета на певній частоті може не бути, або воно може бути дуже малим. Для однозначного виявлення всіх орієнтирів необхідно проводити вимірювання на декількох частотах. У роботі встановлено на скількох частотах потрібно виконати вимірювання й за яким принципом слід вибирати ці частоти.

Практична значимість. Поява цифрових моделей рельєфу місцевості уможливило вирішення завдання орієнтування на місцевості шляхом порівняння радіолокаційних відображень від місцевих предметів з моделями відображень, побудованих за даними цифрових карт рельєфу. У моделей радіолокаційних відображень використовуються математичні очікування величин відображень, на відміну від реальних відображень, що мають випадкові відхилення в рівнях сигналів у залежності від робочої частоти. Зниження дисперсії цих відхилень підвищує точність виділення характерних місцевих предметів (орієнтирів), що використовуються для орієнтації радіолокаційного засобу за відсутності даних від супутникових навігаційних систем.

Ключові слова: *дисперсія, радіолокація, діапазон частот, орієнтир, цифрова модель місцевості*

The manuscript was submitted 24.06.24.